KINARI-BioAssembly Case Study: 3SAQ

Tiffany Q. Liu

May 8, 2012

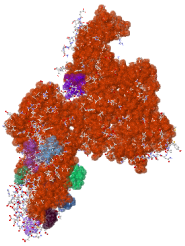

(a) 3SAQ AU

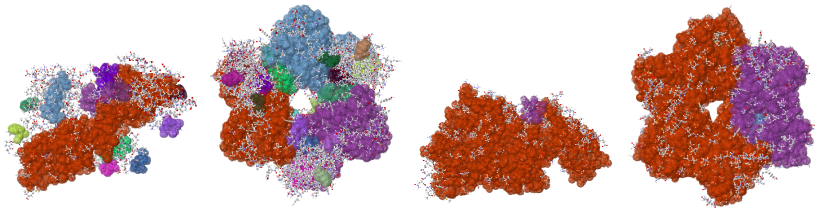

(b) 3SAQ 1/3BU1 (c) 3SAQ BU1 (d) 3SAQ 1/3BU2 (e) 3SAQ BU2

Figure 1: Visualization of rigidity analysis results of 3SAQ from KINARI. The asymmetric unit (a) is composed of two chains, A and B. With the BioAssembly Generator, we can analyze the rigidity of just chain A (b), the trimer made up of three copies of chain A (c), just chain B (d), or the trimer made up of three copies of chain B (e). The colors are randomly assigned by the KINARI rigidity visualizer, and each color represents a different rigid cluster.

3SAQ represents the scaffolding protein D13 of the vaccinia virus, which is also known as the smallpox vaccine. The vaccinia virus, like all poxviruses,

has a viral envelope that surrounds its protein capsid [2]. 3SAQ is used to provide curvature and rigidity to the membranes of immature virions, virus particles outside the cell [1]. In the PDB file for 3SAQ, the asymmetric unit contains two chains, A and B with 576 residues each. There are two biological assemblies that can be generated from these chains. One assembly has three copies of chain A. This is one trimer. The other trimer has three copies of chain B. With the integrated version of KINARI BioAssembly with KINARI Curation and Rigidity Analysis, some interesting features of this viral protein become highlighted. This case is an example of the advantages of being able to generate parts of biological assemblies.

With KINARI, we were able to analyze the rigidty of the 3SAQ asymmetric unit (Fig. 1a), one copy of chain A (Fig. 1b), the biological assembly that is composed of three copies of chain A (Fig. 1c), one copy of chain B (Fig. 1d), and the biological assembly that is composed of three copies of chain B (Fig. 1e). Analyzing the rigidities of chains A and B separately was made possible by the feature of KINARI BioAssembly that allows us to generate portions of biological assemblies.

In Table 1, columns 3 and 4, we can see that overall the rigid clusters increase in numbers by a factor of about three as we move from the one copy of chain A to the entire assembly of three copies of chain A. In columns 5 and 6, we see that the smaller rigid clusters are still increasing by a factor of three as we saw with chain A. However, the largest rigid cluster in the chain B trimer increased from 4562 atoms to 9475 atoms, which suggests that the chemical interactions between the three copies of chain B in the biological assembly have a significant effect on the overally rigidity of the second functional unit in the PDB file. The number of rigid clusters of a particular size increasing by the same factor as the number of copies of the single-chained unit suggests that the computation of rigid clusters could have been done once on one of the units and then mapped to the copied versions of the unit, which could potentially improve the efficiency of the algorithm used for KINARI Rigidity Analysis.

When looking at the rigidity results with the asymmetric unit (column 1), we can see that the chemical interaction between chain A and chain B have a significant effect on the rigidity as well with the largest rigid cluster having 7883 atoms. This result is consistent with the findings that multiple copies of the chain A trimer and the chain B trimer together form a honeycomb lattice, which is what provides the rigidity and structure to the immature virion membrane [2].

Table 1: Rigidity results for 3SAQ - the number of each type of rigid cluster is listed for the asymmetric and biological unit (AU = Asymmetric Unit, BU = Biological Unit). Column 2 is the result from analyzing the asymmetric unit, which contains one copy of A and B each, and columns 3 and 5 are the results from generating only one-third of the biological units listed in columns 4 (three copies of chain A) and 6 (three copies of chain B) respectively.

Size	**AU**	**BU1a**	**BU1**	**BU2a**	**BU2**
3	321	303	911	140	434
4	77	45	132	40	117
5	1462	905	2715	696	2117
6	179	187	561	66	217
7	1	4	12	1	4
11	16	12	36	8	25
12	45	31	93	19	56
13	2	1	3	1	3
15	2	3	9	0	0
16	2	1	3	1	3
19	7	8	24	2	7
22	1	2	6	0	0
25	1	2	6	0	0
33	1	1	3	0	1
38	1	1	0	0	0
42	0	0	3	0	0
48	1	1	3	0	0
71	1	1	3	0	0
98	2	1	3	1	3
104	1	2	6	0	1
2277	0	1	3	0	0
3912	0	0	0	0	1
4562	0	0	0	1	0
7883	1	0	0	0	0
9475	0	0	0	0	1

References

[1] M. Bahar, S. Graham, D. Stuart, and J. Grimes. Insights into the evolution of a complex virus from the crystal structure of vaccinia virus D13. *Structure*, 19:1011–1020, July 2011.

[2] J. K. Hyun, C. Accurso, M. Hijnen, P. Schult, A. Pettikiriarachchi, A. K. Mitra, and F. Coulibaly. Membrane remodeling by the double-barrel scaffolding protein of poxvirus. *PLoS Pathogens*, 7(9), September 2011.